*Progress In Electromagnetics Research, Vol. 129, 69–90, 2012*

# ANALYSIS OF ELECTROMAGNETIC PLANE WAVE SCATTERING FROM 2-D PERIODIC ARRANGEMENTS OF POSTS

**A. Kusiek*, R. Lech, and J. Mazur**

Gdansk University of Technology, 11/12 Narutowicza Street. 80-233, Gdansk, Poland

**Abstract**—In the paper, the analysis of electromagnetic wave scattering from frequency selective surface is presented. The surface is composed of periodically arranged posts. The multimodal scattering matrix of such structure is derived and the transmission and reflection characteristic for the structure with arbitrary plane wave illumination are calculated. The exact full-wave theory based on the mode-matching method is applied to develop an efficient theory to analyze such structures. The validity and accuracy of the approach are verified by comparing the results with those obtained from alternative methods.

## 1. INTRODUCTION

The analysis of plane wave scattering form the frequency selective surface (FSS) composed of periodic arrangements of scatterers is conducted in this paper. The constructive elements of this structure are comparable in size to the operation wavelength and are composed of conducting and dielectric material.

FSSs when multilayered can be utilized as an electromagnetic band structure (EBG) in microwave wavelength range or photonic band structure (PBG) in optical range. Recently, EBGs and PBGs are of great interest due to their extraordinary properties and potential applications, e.g., filters, polarizers, substrates for radiating elements, or optical switches [1–14]. Many numerical techniques have been utilized to investigate band gap structures. The most popular are the cylindrical-harmonic expansion method [15], the finite element method [16], the finite difference method [17], and Fourier modal method [18]. FSSs can also find application in polarizers

*Received 13 April 2012, Accepted 24 May 2012, Scheduled 13 June 2012*

* Corresponding author: Adam Kusiek (adakus@eti.pg.gda.pl).

and polarization rotators to change the polarization state of an electromagnetic wave [19, 20]. Through the utilization of these devices the antennas adopted to receive a single linear polarization (vertical or horizontal) are able to work with both polarizations at the same time.

In this paper, the multimodal scattering matrix of periodic arrangements of metalo-dielectric scatterers is calculated. For the analysis we utilize an efficient numerical technique described in [15, 21, 22], which is based on the transmission matrix (**T**-matrix) approach [23] and uses the lattice sums technique [24]. The technique was previously used to investigate periodic structures employing infinitely long circular cylinders [15, 25]. Here we develop this approach to analyze the structures which are periodic in two directions. In our approach the scattering matrix which relates the incident space-harmonics to the scattered, both reflected and transmitted ones, is defined for a double periodic array. The scattering matrix is expressed in terms of lattice sums characterizing a periodic arrangement of scatterers and the **T**-matrix of periodic unit cell of the structure. In this paper the investigation of cylindrical unit cells employing posts with regular geometry is presented and analytical methods are utilized for the calculation of its **T**-matrix. However, in order to increase the versatility of the approach the combination of analytical and discrete methods can be utilized to investigate posts with irregular shapes enclosed by effective artificial cylinder [26, 27]. One example of such case is investigated further in the article.

## 2. FORMULATION OF THE PROBLEM

The structure under investigation is presented in Fig. 1(a). It is composed of an array of uniformly spaced identical sections situated in a free space and illuminated by a harmonic wave with arbitrary direction. The sections are composed of scatterers of height $d$ and are spaced with distance $h_x$ along $x$ axis and with distance $h_z$ along $z$ axis on the plane $y = 0$. The investigated surface is assumed to be located in rectangular coordinate system.

The aim of the analysis is to find scattering parameters of the investigated structure assuming arbitrary incidence angle of the harmonic wave illuminating FSS. In order to develop the scattering matrix describing the structure the electromagnetic wave is assumed to impinge on the surface with incidence angle ($\theta_{in}$, $\phi_{in}$) from both sides of the structure. The wave illuminating the surface from the upper half-space ($y > 0$) has complex amplitudes $a_1$ for its incoming part and $b_1$ for its reflected part. The wave in the lower half-space ($y < 0$) has therefore complex amplitudes $a_2$ and $b_2$.

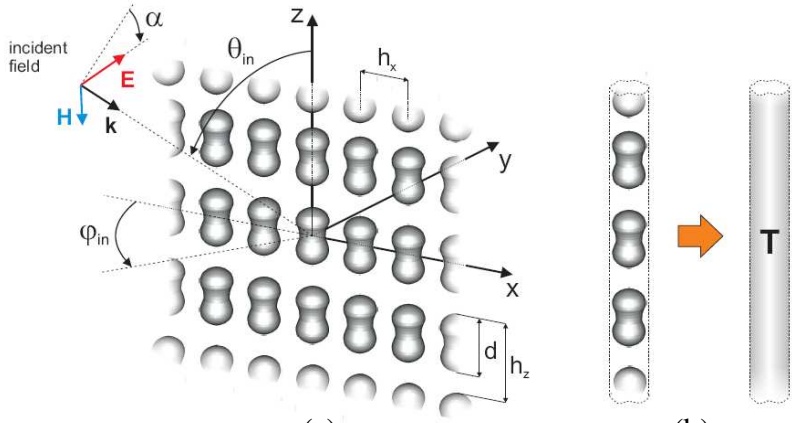


**Figure 1.** Investigated structure of periodically spaced cylinders: (a) View of the structure and (b) **T**-matrix representation of a single unit cell.

Since the structure is periodic in both $x$ and $z$ directions the fields consist of set of space harmonics and the $z$ components of the incident and scattered fields can be described as follows:

$$F_{z,i}^{e(h)} = \sum_p \sum_l a_{1,pl}^{e(h)} e^{j(k_{x,l}x + k_{y,pl}y + k_{z,p}z)} + a_{2,pl}^{e(h)} e^{j(k_{x,l}x - k_{y,pl}y + k_{z,p}z)}, \quad (1)$$

$$F_{z,s}^{e(h)} = \sum_p \sum_l b_{1,pl}^{e(h)} e^{j(k_{x,l}x - k_{y,pl}y + k_{z,p}z)} + b_{2,pl}^{e(h)} e^{j(k_{x,l}x + k_{y,pl}y + k_{z,p}z)}, \quad (2)$$

where $F^e = E$, $F^h = H$, $l = 0, \pm 1, \ldots \pm L$ and $p = 0, \pm 1, \ldots \pm P$ are integers denoting the order of space harmonics, and

$$k_{x,l} = k_{x,0} + \frac{2l\pi}{h_x}, \quad (3)$$

$$k_{z,p} = k_{z,0} + \frac{2p\pi}{h_z}, \quad (4)$$

$$k_{y,pl} = \sqrt{k_0^2 - k_{z,p}^2 - k_{x,l}^2}, \quad (5)$$

where $k_{x,0} = -k_0 \sin\theta_{in} \cos\phi_{in}$, $k_{z,0} = k_0 \cos\theta_{in}$, $a_1^e = \cos\alpha \sin\theta_{in}$, $a_1^h = \sin\alpha \sin\theta_{in}$, and $\alpha$ is an inclination angle of the incoming field on the incidence plane.

The resulting scattering matrix is defined as follows:

$$\begin{bmatrix} \mathbf{b_1} \\ \mathbf{b_2} \end{bmatrix} = \begin{bmatrix} \mathbf{S_{11}} & \mathbf{S_{12}} \\ \mathbf{S_{21}} & \mathbf{S_{22}} \end{bmatrix} \begin{bmatrix} \mathbf{a_1} \\ \mathbf{a_2} \end{bmatrix} = \mathbf{S} \begin{bmatrix} \mathbf{a_1} \\ \mathbf{a_2} \end{bmatrix}, \quad (6)$$

where $\mathbf{S_{ij}}$ $(i,j=1,2)$ are square matrices of $(2\cdot(2L+1)\cdot(2P+1))$ dimensions, $\mathbf{a_i}$ and $\mathbf{b_i}$ $(i=1,2)$ are column vectors of complex amplitudes of $(2\cdot(2L+1)\cdot(2P+1))$ dimension defined as follows:

$$\begin{aligned}\mathbf{a} &= [\mathbf{a}_{-P},\ldots,\mathbf{a}_P]^T,\\ \mathbf{a}_p &= \left[a^e_{p(-L)},\ldots,a^e_{pL},a^h_{p(-L)},\ldots,a^h_{pL}\right],\end{aligned} \tag{7}$$

where $e$ and $h$ denote TM and TE polarization, respectively, and column vector $\mathbf{b}$ is defined analogously.

The scattering nature of any scatterer isolated in the host medium of an infinite extent can be described by its isolated **T**-matrix [23]. **T**-matrix relates the unknown coefficients of the scattered fields with the known coefficients of the incident fields. Its elements are obtained by applying the proper continuity conditions on the surface of scatterer, and depend on the particles size, shape, composition and orientation, but not on the nature of the incident or scattered fields.

The scattered field from the periodic structure can be expressed in terms of **T**-matrix of the single unit cell and the lattice sums characterizing the periodic arrangement of the scatterers. The separation of the analysis of single unit cell greatly simplifies the analytical and numerical procedure for the array problem. In the structure investigated in this paper the single unit cell is composed of scatterers which are periodically arranged along $z$-axis and enclosed by artificial effective cylinder as shown in Fig. 1(b). With this assumption the investigation then boils down to plane wave scattering from a periodic array of effective cylinders.

In this paper, the procedure, which allows to find the scattering matrix of the investigated surface, was divided into three stages. First stage concerns the analysis of periodic arrangements of cylindrical posts illuminated by a single harmonic wave. The aim of this analysis is to find coefficients of the reflected and transmitted fields which are generated in result of the illumination. Second stage concerns developing previous analysis by considering multiple harmonic wave illumination in order to obtain a multimodal scattering matrix of the array. The scattering matrix relates the amplitudes of space harmonics of incident and scattered fields. In the last stage the analysis of a single, isolated cylindrical unit cell is conducted. This analysis is performed in natural basis function of cylinders, that is in cylindrical harmonics. The aim is to find the isolated **T**-matrix of the analyzed object. It is worth noting that the cylindrical unit cell is an effective circular cylinder which can enclose any scatterer with arbitrary shape. In the case of regular geometry of the scatterer, in order to find its isolated **T**-matrix the analytical methods can be utilized [28], while in the case of arbitrary shape the discrete or hybrid methods are used [26, 27].

In this paper, for the sake of brevity, we describe the analysis of the metalo-dielectric or multilayered dielectric scatterers with circular cross-sections. The above mentioned stages will be described in the following subchapters.

### 2.1. Scattered Field from the Periodic Arrangement of Cylindrical Posts

As it was mentioned before, the harmonic wave illuminates the periodic surface form arbitrary direction $(\theta_{in}, \phi_{in})$. For the sake of brevity the case of a single $p'l'$-order space harmonic wave illumination will be described in this chapter. In result the $p'l'$-order reflection and transmission coefficients will be derived here ($p' \in < -P, P >$, $l' \in < -L, L >$). The generalized solution including all space harmonics will be outlined in Chapter 2.2.

The $z$ components of the incident fields in zero-th cylindrical coordinate system $(\rho_0, \phi_0)$ are expressed in cylindrical coordinate system in the following form:

$$F^{e(h)}_{z,\,i,\,p'l'} = \sum_m a^{e(h)}_{p'l'} j^{-m} J_m(k_{\rho,p'}\rho_0) e^{jm(\phi_0 - \alpha_{p'l'})} e^{jk_{z,p'}z}, \tag{8}$$

where $k_{\rho,p'} = \sqrt{k_0^2 - k_{z,p'}^2}$, $\cos\alpha_{p'l'} = -k_{x,l'}/k_{\rho,p'}$, $\mathrm{Im}\{\sin\alpha_{p'l'}\} \geq 0$, $m = 0, \pm 1, \ldots \pm M$ and $J_m(\cdot)$ is a Bessel function of order $m$. The scattered field outside the structure is expressed as a sum of all cylindrical harmonics originating in each cell and moving outwards. The $z$ components of the scattered fields from the periodic arrangement can be expressed in cylindrical coordinate system in the following form:

$$F^{e(h)}_{z,s} = \sum_l e^{jk_{x,l'}lh_x} \sum_p \sum_m c^{e(h)}_{pm} H^{(1)}_m(k_{\rho,p}\rho_l) e^{jm\phi_l} e^{jk_{z,p}z}, \tag{9}$$

where $m = 0, \pm 1, \ldots \pm M$, $k_{\rho,p} = \sqrt{k_0^2 - k_{z,p}^2}$, $H^{(1)}_m(\cdot)$ is a Hankel function of the first kind of order $m$, $c_{pm}$ are the unknown amplitudes of the scattered field in zero-th unit cell and $\rho_l = \sqrt{(x - lh_x)^2 + y^2}$, $\cos\phi_l = \frac{x - lh_x}{\rho_l}$, $\sin\phi_l = \frac{y}{\rho_l}$.

Using the additional theorem for Hankel functions (Graf's formula) given as:

$$H^{(1)}_v(x\rho_l)e^{jm\phi_l} = \begin{cases} \sum\limits_{s=-\infty}^{\infty} J_s(x\rho_0)e^{js\phi_0} H^{(1)}_{s-v}(xhl), & l > 0 \\ \sum\limits_{s=-\infty}^{\infty} J_s(x\rho_0)e^{js\phi_0}(-1)^{s-v} H^{(1)}_{s-v}(xh|l|), & l < 0 \end{cases} \tag{10}$$

for $l = 0$, $H_v^{(1)}(x\rho_0)e^{jv\phi_0}$, the scattered field in zero-th unit cell can be expressed as follows:

$$F_{z,s}^{e(h)} = \sum_p \sum_m c_{pm}^{e(h)} e^{jk_{z,p}z} \left[ e^{jm\phi_0} H_m^{(1)}(k_{\rho,p}\rho_0) + \sum_{l=1}^{L} \sum_s e^{js\phi_0} J_s(k_{\rho,p}\rho_0) H_{s-m}^{(1)}(k_{\rho,p}h_x l) \left( e^{jk_{x,0}lh_x} + (-1)^{s-m} e^{-jk_{x,0}lh_x} \right) \right]. \quad (11)$$

The total field in the vicinity of zero-th unit cell is expressed by:

$$F_{z,tot}^{e(h)} = \sum_p \sum_s J_s(k_{\rho,p}, \rho_0) e^{js\phi_0} \left( j^{-s} e^{-js\alpha_{p'l'}} a_{p'l'}^{e(h)} \delta_{pp'} + \sum_m L_{sm}(k_{\rho,p}h, k_{x,0}h_x) c_{pm}^{e(h)} \right) + \sum_p \sum_m H_m^{(1)}(k_{\rho,p}\rho_0) e^{jm\phi_0} c_{pm}^{e(h)}, \quad (12)$$

where $\delta_{pp'} = 1$ for $p = p'$ and $\delta_{pp'} = 0$ otherwise. $L_{sm}(k_{\rho,p}h, k_{x,0}h_x)$ is $(s-m)$-th order lattice sum written as follows:

$$L_{sm}(k_\rho h, k_x h) = \sum_{l=1}^{L} H_{s-m}^{(1)}(k_\rho hl) \left( e^{jk_x lh} + (-1)^{s-m} e^{-jk_x lh} \right). \quad (13)$$

The first term in the right hand side of Equation (12) may be viewed as an incident field impinging on the zero-th unit cell, whereas the second is the scattered field from the cell. Rewriting above equations in matrix form and utilizing the **T**-matrix description of the object one obtains the following relation between the unknown amplitudes of the scattered field $c_{pm}^{e(h)}$ and the incident wave $a_{p'l'}^{e(h)}$:

$$\mathbf{c} = \mathbf{T} \left( \overline{\mathbf{L}} \cdot \mathbf{c} + \overline{\mathbf{P}}^{+} \cdot \mathbf{a}_{\mathbf{p'l'}} \right), \quad (14)$$

where $\mathbf{c}$ is a column vector of the scattered field unknown coefficients of $(2 \cdot (2P+1) \cdot (2M+1))$ dimension defined as follows:

$$\mathbf{c} = [\mathbf{c}_{-P}, \ldots, \mathbf{c}_P]^T,$$
$$\mathbf{c}_p = \left[ c_{p(-M)}^{e}, \ldots, c_{pM}^{e}, c_{p(-M)}^{h}, \ldots, c_{pM}^{h} \right]. \quad (15)$$

Matrix $\overline{\mathbf{L}}$ is a square matrix of $(2 \cdot (2P+1) \cdot (2M+1))$ dimensions arranged as follows

$$\overline{\mathbf{L}} = \mathrm{diag}\left[ \mathbf{L}_{-P}, \ldots, \mathbf{L}_P \right], \quad \mathbf{L}_p = \begin{bmatrix} \mathbf{L_{sm}} & \mathbf{0} \\ \mathbf{0} & \mathbf{L_{sm}} \end{bmatrix}, \quad (16)$$

where $\mathbf{L_{sm}}$ is a square matrix of $(2M+1)$ dimensions whose elements are given by lattice sums defined in Equation (13). $\overline{\mathbf{P}}$ is a matrix of

$(2 \cdot (2P+1) \cdot (2M+1)) \times (2 \cdot (2P+1) \cdot (2L+1))$ dimensions of the following form:

$$\begin{aligned} \overline{\mathbf{P}}^{\pm} &= \operatorname{diag}\left[\overline{\mathbf{P}}^{\pm}_{-P} \ldots \overline{\mathbf{P}}^{\pm}_{P}\right], \\ \overline{\mathbf{P}}^{\pm}_{p} &= \begin{bmatrix} \mathbf{P}^{\pm(e)}_{p} & \mathbf{0} \\ \mathbf{0} & \mathbf{P}^{\pm(h)}_{p} \end{bmatrix}, \end{aligned} \tag{17}$$

$$\begin{aligned} \left[\mathbf{P}^{\pm(e)}_{p}\right]_{ml} &= \left((j)^{-m} e^{\pm jm\alpha_{pl}}\right), \\ \left[\mathbf{P}^{\pm(h)}_{p}\right]_{ml} &= \left(\frac{j}{\eta}(j)^{-m} e^{\pm jm\alpha_{pl}}\right), \end{aligned} \tag{18}$$

and $\mathbf{a}_{\mathbf{p'l'}}$ is a column vector of excitation of $(2 \cdot (2P+1) \cdot (2L+1))$ dimension with non-zero element at $p'l'$ position. Matrix $\overline{\mathbf{P}}$ transforms $pl$-order space harmonic into $m$-th order cylindrical wave. $\mathbf{T}$ is a square matrix of $(2 \cdot (2P+1) \cdot (2M+1))$ dimensions and for conducting and dielectric periodic cylinder is defined in Chapter 2.3.

Solving Equation (14) one obtains the unknown coefficients of the scattered field $c_{pm}$ as:

$$\mathbf{c} = \overline{\overline{\mathbf{T}}} \cdot \overline{\mathbf{P}}^{+} \cdot \mathbf{a}_{\mathbf{p'l'}}, \tag{19}$$

where $\overline{\overline{\mathbf{T}}}$ is called aggregated transmission matrix and is defined as:

$$\overline{\overline{\mathbf{T}}} = \left(\mathbf{I} - \mathbf{T}\overline{\mathbf{L}}\right)^{-1} \mathbf{T}. \tag{20}$$

Since the scattered field defined in Equation (12) is only valid in the vicinity of zero-th unit cell, it cannot be applied when the observation point is located far from it. To derive the scattered field the recurrence formula and Fourier integral representation for Hankel functions need to be utilized [29].

The reflection and transmission coefficient for $p'l'$-order space harmonic can be calculated using following formula:

$$\mathbf{b}_{\mathbf{1}p'l'} = \mathbf{U}^{+} \cdot \overline{\overline{\mathbf{T}}} \cdot \overline{\mathbf{P}}^{+} \cdot \mathbf{a}_{\mathbf{p'l'}}, \tag{21}$$

$$\mathbf{b}_{\mathbf{2}p'l'} = \delta_{p'l'} + \mathbf{U}^{-} \cdot \overline{\overline{\mathbf{T}}} \cdot \overline{\mathbf{P}}^{+} \cdot \mathbf{a}_{\mathbf{p'l'}}, \tag{22}$$

where matrix $\mathbf{U}^{\pm}$ is of $(2 \cdot (2P+1) \cdot (2L+1)) \times (2 \cdot (2P+1) \cdot (2M+1))$ dimensions and is of a following form:

$$\mathbf{U}^{\pm} = \operatorname{diag}\left[\mathbf{U}^{\pm}_{-P}, \ldots, \mathbf{U}^{\pm}_{P}\right], \tag{23}$$

$$\mathbf{U}^{\pm}_{p} = \begin{bmatrix} \overline{\mathbf{U}}^{\pm}_{p} & \mathbf{0} \\ \mathbf{0} & \overline{\mathbf{U}}^{\pm}_{p} \end{bmatrix}, \tag{24}$$

$$\left[\overline{\mathbf{U}}_p^{\pm}\right]_{lm} = \frac{2(-j)^m}{k_{\rho,p}h_x \sin\alpha_{pl}} e^{\pm jm\alpha_{pl}}, \tag{25}$$

$$\cos\alpha_{pl} = -\frac{k_{x,l}}{k_{\rho,p}}, \quad \mathrm{Im}\{\sin\alpha_{pl}\} \geq 0, \tag{26}$$

$\mathbf{b_1}_{p'l'}$ and $\mathbf{b_2}_{p'l'}$ are column vectors consisting of any $pl$-order space harmonic reflection and transmission coefficients calculated for the $p'l'$-order space harmonic excitation.

### 2.2. Multimodal Scattering Matrix of the Periodic Surface

In order to calculate multimodal scattering matrix of analyzed periodic surface the incident field needs to illuminate structure from both sides and contain all space harmonics ($p = 0, \pm1, \ldots, \pm P$, $l = 0, \pm1, \ldots, \pm L$). Following the analysis presented in previous chapter the elements of scattering matrix can be calculated as follows:

$$\mathbf{S_{11}} = \mathbf{U}^+ \cdot \overline{\overline{\mathbf{T}}} \cdot \overline{\mathbf{P}}^+, \tag{27}$$

$$\mathbf{S_{12}} = \mathbf{I} + \mathbf{U}^+ \cdot \overline{\overline{\mathbf{T}}} \cdot \overline{\mathbf{P}}^-, \tag{28}$$

$$\mathbf{S_{21}} = \mathbf{I} + \mathbf{U}^- \cdot \overline{\overline{\mathbf{T}}} \cdot \overline{\mathbf{P}}^+, \tag{29}$$

$$\mathbf{S_{22}} = \mathbf{U}^- \cdot \overline{\overline{\mathbf{T}}} \cdot \overline{\mathbf{P}}^-. \tag{30}$$

### 2.3. T-matrix of An Isolated Scatterer

The investigated posts are periodic in $z$-direction and are composed of metallo-dielectric or multilayered dielectric cylindrical sections. The cross-sections of the analyzed structures are presented in Fig. 2. The single section of the metallo-dielectric post is composed of two metallic cylinders of height $h_1$ separated by dielectric one of height $h_2$ and permittivity $\varepsilon_r$. The single section of the multilayered dielectric post is composed of axially stacked $N$ dielectric cylinders with heights $h_1, \ldots, h_N$ and permittivities $\varepsilon_{r1}, \ldots, \varepsilon_{rN}$.

In order to analyze the posts and find their **T**-matrices we distinguish two cylindrical regions of investigation. First region is located within post structure ($\rho \leq R$) while the second is defined outside the post ($\rho > R$).

The $z$-components of total electric and magnetic fields in region II are defined as follows:

$$E_z^{II} = \sum_p \sum_m \left( d^e_{1,pm} J_m(k_{\rho,p}\rho) + d^e_{2,pm} H_m^{(1)}(k_{\rho,p}\rho) \right) e^{j(m\varphi + k_{z,p}z)}, \tag{31}$$

$$H_z^{II} = \sum_p \sum_m \left( \widetilde{d}^h_{1,pm} J_m(k_{\rho,p}\rho) + \widetilde{d}^h_{2,pm} H_m^{(1)}(k_{\rho,p}\rho) \right) e^{j(m\varphi + k_{z,p}z)}, \tag{32}$$

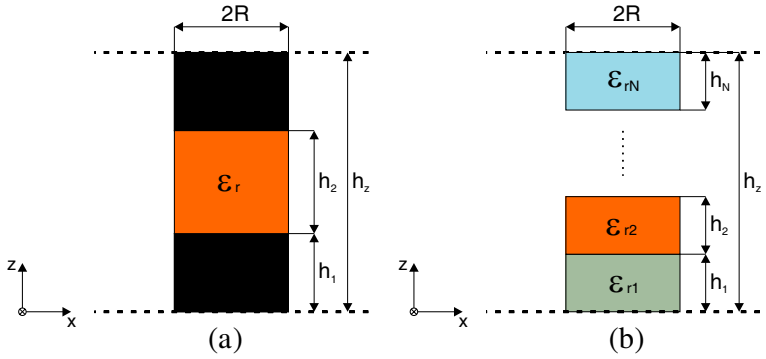


**Figure 2.** Single section of isolated cylinder periodic in the $z$-direction: (a) Metallo-dielectric cylinder and (b) multilayered dielectric cylinder.

where $\widetilde{d} = \frac{j}{\eta_0} d$, $\eta_0 = \sqrt{\mu_0/\varepsilon_0}$ and $d^{e(h)}_{1,pm}$ and $d^{e(h)}_{2,pm}$ are incident and scattered field expansion coefficients, respectively, for $e-$TM, $h-$TE. In region I the $z$-components of electric and magnetic fields are defined as follows:

$$E^I_z = \sum_q \sum_m g^e_{qm} J_m(k^e_{\rho,q}\rho) e^{jm\varphi} f^e_q(z), \tag{33}$$

$$H^I_z = \frac{j}{\eta_0} \sum_q \sum_m g^h_{qm} J_m(k^h_{\rho,q}\rho) e^{jm\varphi} f^h_q(z), \tag{34}$$

where $q = 0, 1, \ldots, Q$, $g^{e(h)}_{qm}$ are field expansion coefficients, wave numbers $k^{e(h)}_{\rho,q}$ and functions $f^{e(h)}_q(\cdot)$ are defined in Appendix A. Utilizing (31)–(34) the $\varphi$ components of electric and magnetic fields in both regions can be found from the following relations:

$$E_\varphi = \frac{1}{k^2_\rho} \left( j\omega\mu \frac{\partial H_z}{\partial \rho} + \frac{1}{\rho} \frac{\partial^2 E_z}{\partial \varphi \partial z} \right), \tag{35}$$

$$H_\varphi = \frac{1}{k^2_\rho} \left( -j\omega\varepsilon \frac{\partial E_z}{\partial_\rho} + \frac{1}{\rho} \frac{\partial^2 H_z}{\partial \varphi \partial z} \right). \tag{36}$$

The aim of the analysis is to determine **T**-matrix representation of the isolated object which relates the incident and scattered field expansion coefficients:

$$\mathbf{d}_2 = \mathbf{T}\mathbf{d}_1, \tag{37}$$

where $\mathbf{d}_{1(2)}$ are column vectors of the form $\mathbf{d}_i = [\mathbf{d}_{i,-P}, \ldots, \mathbf{d}_{i,P}]^T$ and $\mathbf{d}_{i,p} = [d^e_{i,p(-M)}, \ldots, d^e_{i,pM}, d^h_{i,p(-M)}, \ldots, d^h_{i,pM}]$ for $i = 1, 2$.

First step of the analysis consists of formulating field continuity conditions at the surface of cylinder (interface between region I and II $\rho = R$):

$$E_z^{II}(R,\varphi,z) = E_z^{I}(R,\varphi,z), \tag{38}$$

$$E_\varphi^{II}(R,\varphi,z) = E_\varphi^{I}(R,\varphi,z), \tag{39}$$

$$H_z^{II}(R,\varphi,z) = H_z^{I}(R,\varphi,z), \tag{40}$$

$$H_\varphi^{II}(R,\varphi,z) = H_\varphi^{I}(R,\varphi,z), \tag{41}$$

where $\varphi \in [0, 2\pi]$ and $z \in [0, h_z]$. Applying mode matching technique to Equations (38)–(41) we obtain the following matrix equations:

$$\mathbf{M}_{d1}^{e}\mathbf{d}_1 + \mathbf{M}_{d2}^{e}\mathbf{d}_2 = \mathbf{M}_{g}^{e}\mathbf{g}, \tag{42}$$

$$\mathbf{M}_{d1}^{h}\mathbf{d}_1 + \mathbf{M}_{d2}^{h}\mathbf{d}_2 = \mathbf{M}_{g}^{h}\mathbf{g}. \tag{43}$$

For the sake of brevity all matrices in above equations are defined in Appendix B.

In the next step the relation (37) is applied to Equations (42)–(43) resulting in the formula for the **T**-matrix of the investigated post:

$$\mathbf{T} = \left(\mathbf{Z}\mathbf{M}_{d2}^{h} - \mathbf{M}_{d2}^{e}\right)^{-1}\left(\mathbf{M}_{d1}^{e} - \mathbf{Z}\mathbf{M}_{d1}^{h}\right), \tag{44}$$

where:

$$\mathbf{Z} = \mathbf{M}_{g}^{e}(\mathbf{M}_{g}^{h})^{-1}. \tag{45}$$

## 3. CONVERGENCE

In order to perform the calculation of the structure scattering matrix the sums introduced in previous chapter need to be properly truncated. To check the convergence of the presented approach the periodic structure composed of metallic cylinders is considered. The structure dimensions are as follows: $r = 8\,\text{mm}$, $z_1 = 20\,\text{mm}$, $z_2 = 10\,\text{mm}$, spacing $h_x = h_z = 50\,\text{mm}$ and the direction of incident plane wave $\varphi_{in} = 70^\circ$ and $\theta_{in} = 70^\circ$. The frequency dependent scattering parameters characteristics of this structure for different values of eigenfunctions numbers $M$ and $P$ are presented in Fig. 3. The superscripts $a(b)$, where $a$, $b$ =TE,TM indicate that the obtained solution is calculated for $a$ mode with $b$ incident mode. In order to more accurately examine the convergence of the solution the following error criterion is defined:

$$\delta_S = \frac{||S - S^{ref}||}{||S^{ref}||} \cdot 100\%, \qquad \text{where:} \quad ||\cdot|| = \sqrt{\int_{f_{\min}}^{f_{\max}} |\cdot|^2 df}, \tag{46}$$

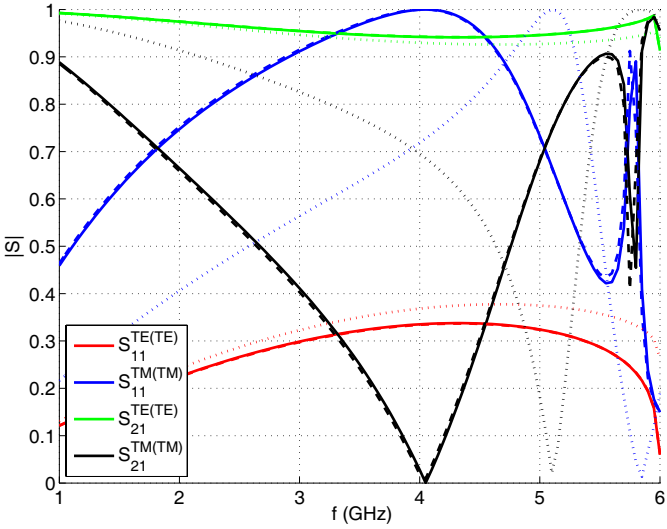


**Figure 3.** Convergence of scattering parameters of metallic periodic structure ($h_x = h_z = 50\,\text{mm}$, $z_1 = 20\,\text{mm}$ and $z_2 = 10\,\text{mm}$) versus number of eigenfunctions: $P = 0$, $M = 1$ — dotted line, $P = 4$, $M = 3$ — dashed line, $P = 10$, $M = 5$ — continuous line.

were $S^{ref}$ are scattering parameters calculated for the highest considered values of $M$ and $P$. The results of this investigation are presented in Table 1.

As can be observed a small number of eigenfunctions ($P = 4$ and $M = 3$) is sufficient for this configuration to obtain rough (the percentage error value of about 1%) but satisfactory results. Assuming the number of eigenfunctions $P = 4$ and $M = 3$, the calculation of single frequency point takes approximately 0.28 s on a MATLAB, Pentium i7 personal computer, while for $P = 10$ and $M = 5$ it takes approximately 1.65 s. Comparing this to the calculation of commercial software ANSYS HFSS the time of single frequency point calculation is 47 s with the number of mesh cells 13046. Despite the undeniable fact of high versatility of commercial software a high speed of the proposed method makes it ideal for use in optimization procedures.

## 4. NUMERICAL RESULTS

A few examples of double periodic structures have been analyzed. The scattering characteristics of these arrays have been calculated. The results are shown for the case of normal incidence as well as for

**Table 1.** Convergence of reflection coefficients $S_{11}^{TE(TE)}$ and $S_{11}^{TM(TM)}$ versus eigenfunctions numbers $P$ and $M$.

| $P$ | $\delta S_{11}^{TE(TE)}$ [%] | | | | $\delta S_{11}^{TM(TM)}$ [%] | | | |
|---|---|---|---|---|---|---|---|---|
| | $M$ | | | | $M$ | | | |
| | 1 | 2 | 3 | 5 | 1 | 2 | 3 | 5 |
| 0 | 5.29 | 4.09 | 4.12 | 4.12 | 9.32 | 9.34 | 9.34 | 9.34 |
| 2 | 5.29 | 4.09 | 4.12 | 4.12 | 1.27 | 1.38 | 1.38 | 1.38 |
| 4 | 2.87 | 1.12 | 1.05 | 1.05 | 1.20 | 1.07 | 1.07 | 1.07 |
| 6 | 3.04 | 0.54 | 0.36 | 0.36 | 1.25 | 1.12 | 1.12 | 1.12 |
| 8 | 3.05 | 0.51 | 0.32 | 0.32 | 0.48 | 0.29 | 0.28 | 0.28 |
| 10 | 3.07 | 0.40 | 0.03 | - | 0.55 | 0.07 | 0.01 | - |

arbitrary angle of incidence. The characteristics are illustrated for power reflection and transmission coefficients of the fundamental space harmonics ($p = 0, l = 0$) versus frequency or for chosen single frequency versus angle of incidence.

For the calculations of the presented examples the number of space harmonics $L = 4$, $P = 6$ with $Q = 2$ (for metallic structures) or $Q = 6$ (for dielectric structures) and number of cylindrical functions $M = 7$ were chosen which was sufficient to obtain convergence of the solution.

In the first and second example the case of normal incidence on the periodic structure of metallic posts is considered. The first structure is composed of infinitely long metallic cylinders of radii $r = 8\,\text{mm}$ arranged with period $h_x = 50\,\text{mm}$. The second structure is composed of metallic cylinders of radii $r = 8\,\text{mm}$ and heights $h_1 = 15\,\text{mm}$, $h_2 = 20\,\text{mm}$ and is arranged with period $h_x = h_z = 50\,\text{mm}$. The power reflection and transmission coefficients are calculated versus frequency for both examples. The results are presented in Fig. 4(a) and Fig. 4(b). Comparing both configurations one can see that the replacement of infinitely long cylinders from first example by periodic cylinders from second example only slightly affects the response of TE wave and has significant influence on TM wave. For TM wave the infinitely long cylinder constitute an inductance while for periodic cylinder an additional parallel capacitance is formed in the gaps between cylinders, which gives rise to a resonance visible in $S_{21}^{TM}$ characteristic in Fig. 4(b). The presented results have been compared with the results obtained from HFSS commercial software obtaining a very good agreement.

The double periodic surface can be utilized to change the polarization state of the transmitted wave (axial ratio AR, polarization

angle $\zeta$ [30]). In the next example a periodic structure composed of thin metallic cylinders of radii $r = 1$ mm with different heights and arranged with period $h_x = h_z = 50$ mm is analyzed for normal incidence of the

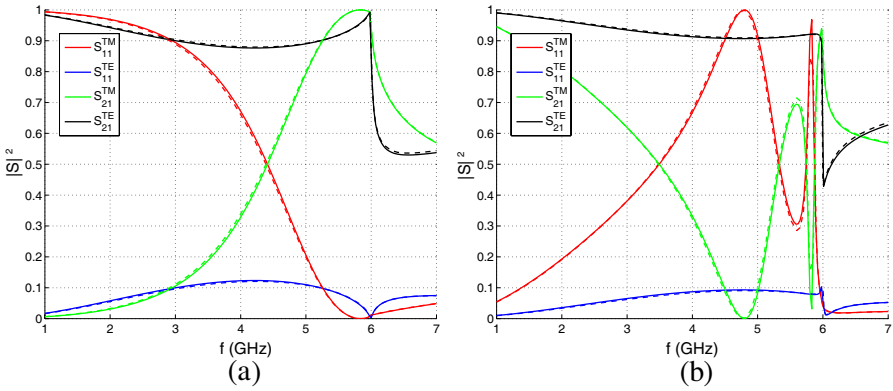


**Figure 4.** Power reflection and transmission coefficients versus frequency for (a) infinitely long metallic cylinders of $r = 8$ mm arranged with period $h_x = 50$ mm and (b) double periodic metallic cylinders of radii $r = 8$ mm and heights $h_1 = 15$ mm, $h_2 = 20$ mm, arranged with period $h_x = h_z = 50$ mm for normal incidence; solid line — our approach, dashed line — HFSS.

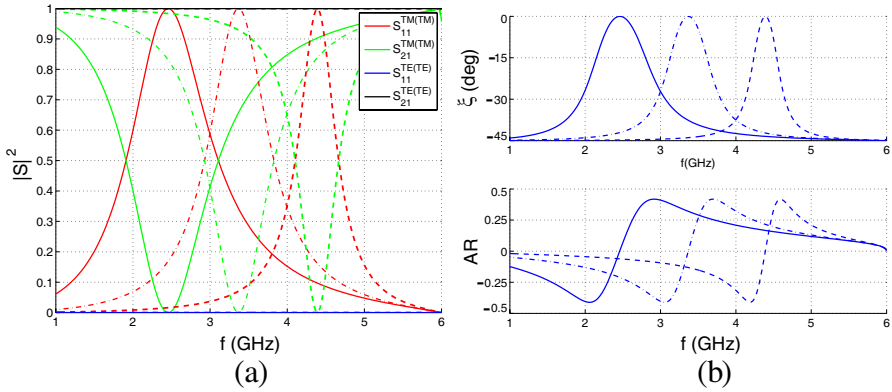


**Figure 5.** Double periodic structure composed of metallic cylinders of radii $r = 1$ mm and different heights (solid line $h_2 = 0.5$ mm, dash-dot line $h_2 = 8$ mm, dashed line $h_2 = 20$ mm), arranged with period $h_x = h_z = 50$ mm for normal incidence (a) power reflection and transmission coefficients versus frequency; (b) polarization parameters (axial ratio AR, polarization angle $\zeta$) of the transmitted wave versus frequency.

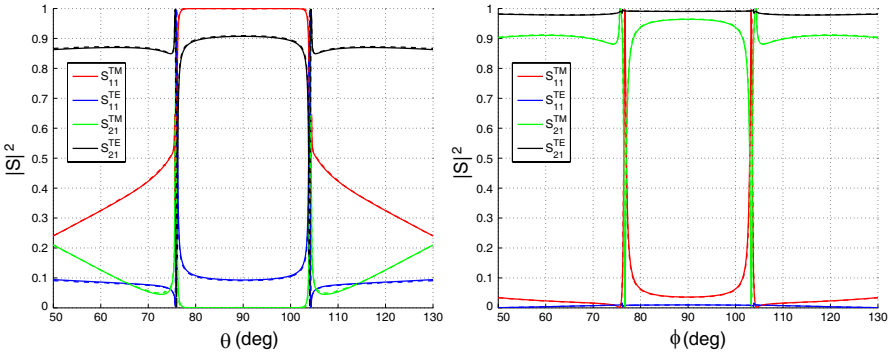


**Figure 6.** Power reflection and transmission coefficients versus angle of incidence $\theta_{in}$ for frequency $f = 4.8\,\text{GHz}$ and angle $\phi_{in} = 90°$. (a) Metallic structure with dimension from Fig. 4(b). (b) Double periodic dielectric structure with single cell composed of 3 layer dielectric cylinder of radii $r = 8\,\text{mm}$, heights $h_1 = 15\,\text{mm}$, $h_2 = 20\,\text{mm}$ and permittivity $\varepsilon_{r1} = 3$, $\varepsilon_{r2} = 1$ and $\varepsilon_{r3} = 3$ arranged with period $h_x = h_z = 50\,\text{mm}$; Solid line — our approach; Dashed line — HFSS.

wave inclined by $\alpha = 45°$ with respect to the cylinder axis. The results are presented in Fig. 5. As can be seen the TE wave is not affected by the structure and by adjusting heights of the cylinders one can control the transmission of the TM wave. For a given height of the posts the TM wave is completely reflected for the selected frequency, thus the only transmitted wave is of TE polarization. In result the structure changes the polarization angle of linearly polarized wave by 45°.

In the next example the metallic structure from Fig. 4(b) is analyzed and the power reflection and transmission coefficients are calculated for frequency $f = 4.8\,\text{GHz}$ versus angle of incidence $\theta_{in}$ with angle $\phi_{in} = 90°$. The results are presented in Fig. 6(a). The dielectric cylinder configuration is considered next. The single cell of the periodic structure consists of 3 layer dielectric cylinder of radius $r = 8\,\text{mm}$, heights $h_1 = 15\,\text{mm}$, $h_2 = 20\,\text{mm}$ and permittivity $\varepsilon_{r1} = 3$, $\varepsilon_{r2} = 1$ and $\varepsilon_{r3} = 3$ arranged with period $h_x = h_z = 50\,\text{mm}$. The power reflection and transmission coefficients are calculated versus angle of incidence $\phi_{in}$ with angle $\theta_{in} = 90°$. The results are presented in Fig. 6(b).

As can be seen from the presented examples for the metallic structure and near normal incidence the complete reflection is obtained for TM wave while TE wave is transmitted through the structure. In the case of dielectric structure both waves are easily transmitted through the structure except for angle about $\pm 14°$ from normal

incidence. Again a very good agreement was obtained between results from presented approach and HFSS commercial software simulations.

In the next example the double periodic configuration of metallic cylinders of radii $r = 10\,\text{mm}$, heights $h_1 = 22.5\,\text{mm}$, $h_2 = 15\,\text{mm}$, arranged with period $h_x = h_z = 60\,\text{mm}$ is investigated for wave incidence angles $\phi_{in} = 70°$ and $\theta_{in} = 70°$. The power reflection and transmission coefficients are calculated versus frequency and presented in Fig. 7(a). The structure can be utilized for changing the polarization state of the transmitted wave. As can be observed from Fig. 7(b) by changing the inclination angle of the incident wave with respect to the axis of cylinders one can change the linearly polarized wave to the wave with circular polarization which occurs for $\alpha = 82°$ where AR=1 and $\zeta$ is undetermined. The results presented in Fig. 7(b) were calculated for frequency $f_0 = 3.59\,\text{GHz}$.

The last example presents the investigation of periodic structure composed of metallic posts with rectangular cross-section as presented in Fig. 8(a). The posts are of dimension $a = 20\,\text{mm}$ and $b = 2\,\text{mm}$ and are arranged with period $h_x = 40\,\text{mm}$. The analysis of the single post enclosed by artificial effective cylinder was performed with the use of FDFD method. In result the **T**-matrix of such post was obtained and then utilized in the procedure of calculating scattering parameters. The power reflection and transmission coefficients are calculated versus post rotation angle. The results for normal plane wave incidence are

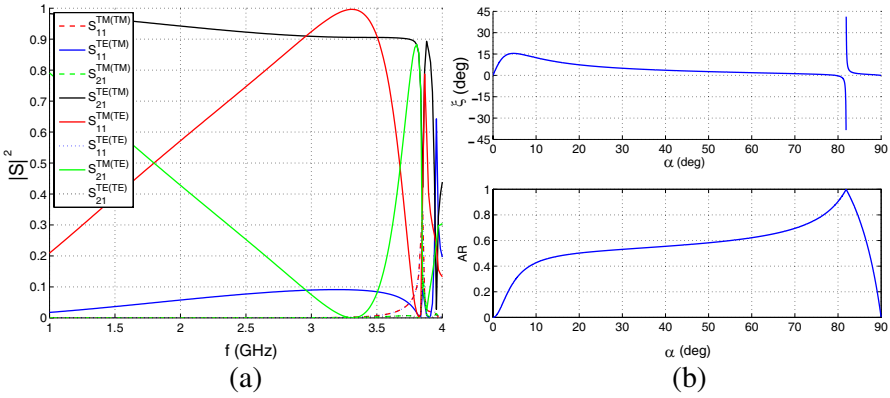


**Figure 7.** Double periodic structure composed of metallic cylinders of radii $r = 10\,\text{mm}$, heights $h_1 = 22.5\,\text{mm}$ and $h_2 = 15\,\text{mm}$, arranged with period $h_x = h_z = 60\,\text{mm}$ for incidence $\phi_{in} = 70°$ and $\theta_{in} = 70°$. (a) Power reflection and transmission coefficients versus frequency. (b) Polarization parameters (axial ratio AR, rotation angle $\zeta$) of the transmitted wave versus inclination angle $\alpha$.

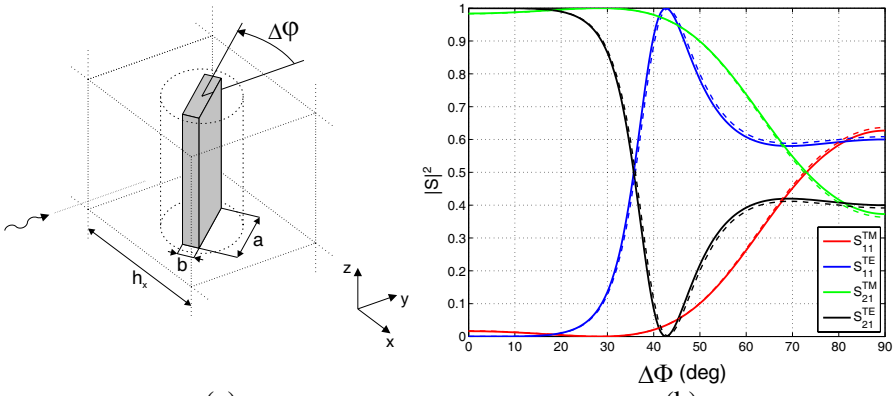


**Figure 8.** Periodic structure composed of infinitely long metallic cylinders with rectangular cross-section ($a = 20\,\text{mm}$, $b = 2\,\text{mm}$), arranged with period $h_x = 40\,\text{mm}$ for incidence $\phi_{in} = 90°$ and $\theta_{in} = 90°$. (a) View of the structure. (b) Power reflection and transmission coefficients versus posts rotation angle $\Delta_\varphi$ at $f_0 = 6.6\,\text{GHz}$; Solid line — our approach; Dashed line — HFSS.

presented in Fig. 8(b). As can be seen the utilization of inhomogeneous scatterers allows one to control the signal transmission by means of their rotation in the array. It is worth noting that for this example the single frequency calculation time takes approximately 1 s (with 4800 mesh cells in unit cell region) while HFSS needs for the same task 30 s with the number of mesh cells 8290. Additional advantage of our approach, which is utilized in this example and speeds up the algorithm, is the possibility of calculating the **T**-matrix of the post only once, for an arbitrary post rotation angle, and then use the analytical formulas to calculate **T**-matrix for rotated object.

## 5. CONCLUSION

The analysis of electromagnetic wave scattering from double periodic frequency selective surface has been presented in this paper. The multimodal scattering matrix of such structure is derived using the efficient numerical model based on the transmission matrix approach and lattice sums technique. The transmission and reflection characteristic for the structure with arbitrary plane wave illumination were calculated for several presented examples. The validity and accuracy of the approach are verified by comparing the results with those obtained from alternative methods.

## ACKNOWLEDGMENT

This work was supported by the Polish Ministry of Science and Higher Education (National Science Center) under Contract N515 501740, decision No 5017/B/T02/2011/40 and under funding for Statutory Activities for ETI Gdansk University of Technology.

## APPENDIX A.

In Equations (33) and (34) wave numbers $k_{\rho,q}^{e(h)}$ and functions $f_q^{e(h)}(\cdot)$ are defined individually for each considered post from Fig. 2 and take a following form:

- metallic cylinder (see Fig. 2(a))

$$f_q^e(z) = \cos(k_{z,q}(z - z_1)), \qquad f_q^h(z) = \sin(k_{z,q}(z - z_1)), \quad \text{(A1)}$$

where: $z \in [z_1, z_2]$, $z_1 = h_1$, $z_2 = h_1 + h_2$, $k_{z,q} = (q\pi)/h_2$ and $k_{\rho,q} = \sqrt{k_0^2\varepsilon_r - k_{z,q}^2}$,

- dielectric cylinder (see Fig. 2(b))

$$f_q^e(z) = \sum_{n=1}^{N} \left( g_{1q}^{e,n} \cos(k_{z,qn}^e z^n) + g_{2q}^{e,n} \sin(k_{z,qn}^e z^n) \right) \psi_n(z), \quad \text{(A2)}$$

$$f_q^h(z) = \sum_{n=1}^{N} \left( g_{1q}^{h,n} \sin(k_{z,qn}^h z^n) + g_{2q}^{h,n} \cos(k_{z,qn}^h z^n) \right) \psi_n(z), \quad \text{(A3)}$$

where $k_{z,qn}^{e(h)} = \sqrt{k_0^2\varepsilon_{rn} - (k_{\rho,q}^{e(h)})^2}$, $z^n = z - z_n$, $z_n = z_{n-1} + h_n$, $z_0 = 0$, $N$ is the number of dielectric layers and function $\psi_n(z)$ is defined as follows:

$$\psi_n(z) = \begin{cases} 1 & z_n \le z < z_{n+1} \\ 0 & \text{otherwise} \end{cases}. \quad \text{(A4)}$$

The wave number $k_{\rho,q}^{e(h)}$ and coefficients $g_1^{e(h),n}$, $g_2^{e(h),n}$ are unknown and have to be determined. Satisfying the boundary continuity conditions:

$$\varepsilon_n E_z(z)|_{z=z_n^-} = \varepsilon_{n+1} E_z(z)|_{z=z_n^+}, \quad \text{(A5)}$$

$$\frac{\partial E_z(z)}{\partial z}|_{z=z_n^-} = \frac{\partial E_z(z)}{\partial z}|_{z=z_n^+}, \quad \text{(A6)}$$

$$\mu_n H_z(z)|_{z=z_n^-} = \mu_{n+1} H_z(z)|_{z=z_n^+}, \quad \text{(A7)}$$

$$\frac{\partial H_z(z)}{\partial z}|_{z=z_n^-} = \frac{\partial H_z(z)}{\partial z}|_{z=z_n^+}, \quad \text{(A8)}$$

for each $n = 1, \ldots, N$ we are obtaining the transfer matrix $\mathbf{T}_q^{e(h)}$ [31] defined as:

$$\mathbf{T}_q^{e(h)} = \prod_{n=1}^{N} \mathbf{T}_n^{e(h)}, \tag{A9}$$

where

$$\mathbf{T}_{qn}^{e} = \begin{bmatrix} \cos(k_{zqn}^{e} h_n) & -\frac{k_{z,qn}^{e}}{\varepsilon_n} \sin(k_{z,qn}^{e} h_n) \\ \frac{\varepsilon_n}{k_{z,qn}^{e}} \sin(k_{z,qn}^{e} h_n) & \cos(k_{z,qn}^{e} h_n) \end{bmatrix}, \tag{A10}$$

$$\mathbf{T}_{qn}^{h} = \begin{bmatrix} \cos(k_{z,qn}^{e} h_n) & \frac{1}{k_{z,qn}^{e}} \sin(k_{z,qn}^{e} h_n) \\ -k_{zqn}^{e} \sin(k_{z,qn}^{e} h_n) & \cos(k_{z,qn}^{e} h_n) \end{bmatrix}. \tag{A11}$$

Now, by applying Floquet theorem we are obtaining the following system of homogeneous equations:

$$\left( \mathbf{T}_q^{e(h)} - e^{(jk_0 \cos\theta_0 h_z)} \mathbf{I} \right) \mathbf{g}_q^{e(h)} = 0, \tag{A12}$$

where $\mathbf{I}$ is the unit matrix of size $2 \times 2$, $\mathbf{g}_q^{e} = [\beta_1 g_{1q}^{e}, \varepsilon_{r1} g_{2q}^{e}]^T$ and $\mathbf{g}_q^{h} = [g_{1q}^{h}, \beta_1 g_{2q}^{h}]^T$. The wavenumbers $k_{\rho,q}^{e(h)}$ are the roots of the equation:

$$\det \left( \mathbf{T}_q^{e(h)} - e^{(jk_0 \cos\theta_0 h_z)} \mathbf{I} \right) = 0, \tag{A13}$$

Finally, solving (A12) for each $k_{\rho,q}^{e(h)}$ the column vectors $\mathbf{g}_q^{e(h)}$ are obtained.

## APPENDIX B.

In Equation (44) matrices $\mathbf{M}_{d1}^{E(H)}$, $\mathbf{M}_{d2}^{E(H)}$ and $\mathbf{M}_{g}^{E(H)}$ take a general form:

$$\mathbf{M}_{\alpha}^{E(H)} = \mathrm{diag}[\mathbf{M}_{\alpha,-M}^{E(H)}, \ldots, \mathbf{M}_{\alpha,M}^{E(H)}],$$

where $\alpha = \{d1, d2, g\}$,

$$\mathbf{M}_{\alpha,m}^{E} = \begin{bmatrix} \mathbf{I}_{\alpha}^{E_z^e} \mathbf{M}_{\alpha,m}^{E_z^e} & \mathbf{0} \\ \mathbf{I}_{\alpha}^{E_\varphi^e} \mathbf{M}_{\alpha,m}^{E_\varphi^e} & \mathbf{I}_{\alpha}^{E_\varphi^h} \mathbf{M}_{\alpha,m}^{E_\varphi^h} \end{bmatrix}, \quad \mathbf{M}_{\alpha,m}^{H} = \begin{bmatrix} \mathbf{I}_{\alpha}^{H_\varphi^e} \mathbf{M}_{\alpha,m}^{H_\varphi^e} & \mathbf{I}_{\alpha}^{H_\varphi^h} \mathbf{M}_{\alpha,m}^{H_\varphi^h} \\ \mathbf{0} & \mathbf{I}_{\alpha}^{H_z^h} \mathbf{M}_{\alpha,m}^{H_z^h} \end{bmatrix},$$

matrices of electric and magnetic fields take form:

$$\left[\mathbf{M}_{\alpha,m}^{E_z^e}\right]_{pp} = Z_m(k_{\rho p} R), \qquad \left[\mathbf{M}_{\alpha,m}^{H_z^h}\right]_{pp} = j/\eta_0 Z_m(k_{\rho p} R),$$

$$\left[\mathbf{M}_{\alpha,m}^{E_\varphi^e}\right]_{pp} = \frac{jm}{k_{\rho p}^2 R} Z_m(k_{\rho p} R), \qquad \left[\mathbf{M}_{\alpha,m}^{E_\varphi^h}\right]_{pp} = \frac{-\omega\mu_0}{\eta_0 k_{\rho p}} Z'_m(k_{\rho p} R),$$

$$\left[\mathbf{M}_{\alpha,m}^{H_\varphi^e}\right]_{pp} = \frac{-j\omega\varepsilon_0}{k_{\rho p}} Z'_m(k_{\rho p} R), \qquad \left[\mathbf{M}_{\alpha,m}^{H_\varphi^h}\right]_{pp} = \frac{-m}{\eta_0 k_{\rho p}^2 R} Z_m(k_{\rho p} R)$$

and matrices of integrals are defined as follows:

$$\left[\mathbf{I}^{E_z^e}_{B1(B2)}\right]_{pp} = \left[\mathbf{I}^{E_\varphi^h}_{B1(B2)}\right]_{pp} = h_z, \qquad \left[\mathbf{I}^{E_\varphi^h}_{B1(B2)}\right]_{pp} = jk_{zp}h_z,$$

$$\left[\mathbf{I}^{H_z^h}_{B1(B2)}\right]_{qp} = \int_0^{h_z} f_q^h(z)e^{jk_{zp}z}dz, \qquad \left[\mathbf{I}^{H_\varphi^h}_{B1(B2)}\right]_{qp} = \int_0^{h_z} jk_{zp}f_q^h(z)e^{jk_{zp}z}dz,$$

$$\left[\mathbf{I}^{E_z^e}_{A}\right]_{pq} = \int_0^{h_z} f_q^e(z)e^{-jk_{zp}z}dz, \qquad \left[\mathbf{I}^{E_\varphi^h}_{A}\right]_{pq} = \int_0^{h_z} f_q^h(z)e^{-jk_{zp}z}dz,$$

$$\left[\mathbf{I}^{E_\varphi^h}_{A}\right]_{pq} = \int_0^{h_z} \frac{\partial f_q^e(z)}{\partial z}e^{-jk_{zp}z}dz, \qquad \left[\mathbf{I}^{H_\varphi^h}_{A}\right]_{qq'} = \int_0^{h_z} f_q^e(z)f_{q'}^h(z)dz,$$

$$\left[\mathbf{I}^{H_\varphi^e}_{A}\right]_{qq'} = \int_0^{h_z} \varepsilon_r(z)f_q^e(z)f_{q'}^e(z)dz, \qquad \left[\mathbf{I}^{H_z^h}_{A}\right]_{qq'} = \int_0^{h_z} f_q^h(z)f_{q'}^h(z)dz.$$

## REFERENCES


1. Wu, T. K., *Frequency Selective Surfaces and Grid Array*, Wiley, New York, 1995.
2. Munk, B. A., *Frequency Selective Surfaces: Theory and Design*, Wiley, New York, 2000.
3. Khromova, I., I. Ederra, R. Gonzalo, and B. P. de Hon, "Symmetrical pyramidal horn antennas based on EBG structures," *Progress In Electromagnetics Research B*, Vol. 29, 1–22, 2011.
4. Huang, M.-J., M.-Y. Lv, and Z. Wu, "Transmission upper bound of planar single-layer frequency selective surface," *Progress In Electromagnetics Research B*, Vol. 23, 15–38, 2010.
5. Xie, H.-H., Y.-C. Jiao, L.-N. Chen, and F.-S. Zhang, "An effective analysis method for EBG reducing patch antenna coupling," *Progress In Electromagnetics Research Letters*, Vol. 21, 187–193, 2011.
6. Veysi, M. and M. Shafaee, "EBG frequency response tuning using an adjustable air-gap," *Progress In Electromagnetics Research Letters*, Vol. 19, 31–39, 2010.
7. Xie, H.-H., Y.-C. Jiao, L.-N. Chen, and F.-S. Zhang, "Omnidirectional horizontally polarized antenna with EBG cavity for gain enhancement," *Progress In Electromagnetics Research Letters*, Vol. 15, 79–87, 2010.

8. Ren, L.-S., Y.-C. Jiao, J.-J. Zhao, and F. Li, "RCS reduction for a FSS-backed reflectarray using a ring element," *Progress In Electromagnetics Research Letters*, Vol. 26, 115–123, 2011.
9. Kong, Y. W. and S. T. Chew, "EBG-based dual mode resonator filter," *IEEE Microwave and Wireless Components Letters*, Vol. 14, No. 3, 124–126, Mar. 2004.
10. Coccioli, R., F.-R. Yang, K.-P. Ma, and T. Itoh, "Aperture-coupled patch antenna on UC-PBG substrate," *IEEE Transactions on Microwave Theory and Techniques*, Vol. 47, No. 11, 2123–2130, Nov. 1999.
11. Jandieri, V., K. Yasumoto, and Y.-K. Cho, "Rigorous analysis of electromagnetic scattering by cylindrical EBG structures," *Progress In Electromagnetics Research*, Vol. 121, 317–342, 2011.
12. Kim, S.-H., T. T. Nguyen, and J.-H. Jang., "Reflection characteristics of 1-D EBG ground plane and its application to a planar dipole antenna," *Progress In Electromagnetics Research*, Vol. 120, 51–66, 2011.
13. Wang, X., M. Zhang, and S.-J. Wang, "Practicability analysis and application of PBG structures on cylindrical conformal microstrip antenna and array," *Progress In Electromagnetics Research*, Vol. 115, 495–507, 2011.
14. Lin, S. Y. and J. G. Fleming, "A three-dimensional optical photonic crystal," *J. Lightwave Technol.*, Vol. 17, 1944–1947, 1999.
15. Kushta, T. and K. Yasumoto, "Electromagnetic scattering from periodic arrays of two circular cylinders per unit cell," *Progress In Electromagnetics Research*, Vol. 29, 69–85, 2000.
16. Pelosi, G., A. Cocchi, and A. Monorchio, "A hybrid FEM-based procedure for the scattering from photonic crystals illuminated by a Gaussian beam," *IEEE Transactions on Antennas and Propagation*, Vol. 48, 973–980, Jun. 2000.
17. Yang, H. Y. D., "Finite difference analysis of 2-D photonic crystals," *IEEE Transactions on Microwave Theory and Techniques*, Vol. 44, 2688–2695, Dec. 1996.
18. Frezza, F., L. Pajewski, and G. Schettini, "Characterization and design of two-dimensional electromagnetic band-gap structures by use of a full-wave method for diffraction gratings," *IEEE Transactions on Microwave Theory and Techniques*, Vol. 51, No. 3, 941–951, Mar. 2003.
19. Wasylkiwskyj, W., "On the transmission coefficient of an infinite grating of parallel perfectly conducting circular cylinders," *IEEE*

*Transactions on Antennas and Propagation*, Vol. 19, No. 5, 704–708, Sep. 1971.

20. Saleh, A. A. M., "An adjustable quasi-optical bandpass filter — Part I: Theory and design formulas," *IEEE Transactions on Microwave Theory and Techniques*, Vol. 22, No. 7, 728–734, Jul. 1974.
21. Yasumoto, K., H. Toyama, and T. Kushta, "S-matrix solution of electromagnetic scattering from periodic arrays of metallic cylinders with arbitrary cross section," *IEEE Antennas and Wireless Propagation Letters*, Vol. 3, 41–44, 2004.
22. Yasumoto, K., H. Toyama, and T. Kushta, "Accurate analysis of two-dimensional electromagnetic scattering from multilayered periodic arrays of circular cylinders using lattice sums technique," *IEEE Transactions on Antennas and Propagation*, Vol. 52, No. 10, 2603–2611, Oct. 2004.
23. Tsang, L., J. A. Kong, and K.-H. Ding, *Scattering of Electromagnetic Waves: Theories and Applications*, John Wiley and Sons, INC., New York, 2000.
24. Yasumoto, K. and K. Yoshitomi, "Efficient calculation of lattice sums for freespace periodic Green function," *IEEE Transactions on Antennas and Propagation*, Vol. 47, No. 6, 1050–1055, Jun. 1999.
25. Lech, R. and J. Mazur, "Electromagnetic curtain effect and tunneling properties of multilayered periodic structures," *IEEE Antennas and Wireless Propagation Letters*, Vol. 7, 201–205, 2008.
26. Kusiek, A. and J. Mazur, "Analysis of scattering from arbitrary configuration of cylindrical objects using hybrid finite-difference mode-matching method," *Progress In Electromagnetics Research*, Vol. 97, 105–127, 2009.
27. Kusiek, A. and J. Mazur, "Application of hybrid finite-difference mode-matching method to analysis of structures loaded with axially-symmetrical posts," *Microwave and Optical Technology Letters*, Vol. 53, No. 1, 189–194, Jan. 2011.
28. Lech, R. and J. Mazur, "Analysis of circular cavity with cylindrical objects," *IEEE Transactions on Microwave Theory and Techniques*, Vol. 55, No. 10, 2115–2123, Oct. 2007.
29. Yasumoto, K., *Electromagnetic Theory and Applications for Photonic Crystals*, CRC Press, New-York, 2005.
30. Stutzman, W., *Polarization in Electromagnetic Systems*, Artech House, 1993.

31. Mrozowski, M. and J. Mazur, "General analysis of a parallel-plate waveguide inhomogeneously filled with gyromagnetic media," *IEEE Transactions on Microwave Theory and Techniques*, Vol. 34, No. 4, 388–395, Apr. 1986.